

Patterns of floodplain sediment deposition along the regulated lower Roanoke River, North Carolina: Annual, decadal, centennial scales



C.R. Hupp^{a,*}, E.R. Schenk^a, D.E. Kroes^b, D.A. Willard^c, P.A. Townsend^d, R.K. Peet^e

^a U.S. Geological Survey, 430 National Center, Reston, VA 20192, USA

^b U.S. Geological Survey, Louisiana Water Science Center, Baton Rouge, LA 70816, USA

^c U.S. Geological Survey, 926A National Center, Reston, VA 20192, USA

^d Department of Forest and Wildlife Ecology, University of Wisconsin, Madison, WI, 53706, USA

^e Department of Biology, University of North Carolina, Chapel Hill, NC 27599, USA

ARTICLE INFO

Article history:

Received 18 March 2014

Received in revised form 15 October 2014

Accepted 18 October 2014

Available online 28 October 2014

Keywords:

Floodplain sedimentation

Legacy sediment

Regulated flow

Dam impacts

GIS model

Dendrogeomorphology

ABSTRACT

The lower Roanoke River on the Coastal Plain of North Carolina is not embayed and maintains a floodplain that is among the largest on the mid-Atlantic Coast. This floodplain has been impacted by substantial aggradation in response to upstream colonial and post-colonial agriculture between the mid-eighteenth and mid-nineteenth centuries. Additionally, since the mid-twentieth century stream flow has been regulated by a series of high dams. We used artificial markers (clay pads), tree-ring (dendrogeomorphic) techniques, and pollen analyses to document sedimentation rates/amounts over short-, intermediate-, and long-term temporal scales, respectively. These analyses occurred along 58 transects at 378 stations throughout the lower river floodplain from near the Fall Line to the Albemarle Sound. Present sediment deposition rates ranged from 0.5 to 3.4 mm/y and 0.3 to 5.9 mm/y from clay pad and dendrogeomorphic analyses, respectively. Deposition rates systematically increased from upstream (high banks and floodplain) to downstream (low banks) reaches, except the lowest reaches. Conversely, legacy sediment deposition (A.D. 1725 to 1850) ranged from 5 to about 40 mm/y, downstream to upstream, respectively, and is apparently responsible for high banks upstream and large/wide levees along some of the middle stream reaches. Dam operations have selectively reduced levee deposition while facilitating continued backswamp deposition. A GIS-based model predicts 453,000 Mg of sediment is trapped annually on the floodplain and that little watershed-derived sediment reaches the Albemarle Sound. Nearly all sediment in transport and deposited is derived from the channel bed and banks. Legacy deposits (sources) and regulated discharges affect most aspects of present fluvial sedimentation dynamics. The lower river reflects complex relaxation conditions following both major human alterations, yet continues to provide the ecosystem service of sediment trapping.

Published by Elsevier B.V.

1. Introduction

The action of flowing water, typically stream flow, mediates fluvial geomorphic processes and provides for the development of bottomland landforms, including the floodplain, which is a dominant fluvial feature in the riparian landscape (Osterkamp and Hupp, 1984; Nanson and Croke, 1992; Hupp and Osterkamp, 1996). Much geomorphic research in fluvial systems focuses on patterns and controls on the erosion, entrainment, transport, deposition, and storage of sediment. Floodplains, major sites for sediment trapping, achieve their greatest North American extent on the lowland Coastal Plain Physiographic Province that includes large parts of southeastern United States (Hupp, 2000). Coastal Plain floodplains are the last substantial areas for sediment, nutrient, and carbon storage before reaching tidewater and critical

estuarine ecosystems. Quantification of temporal and spatial aspects of sediment storage is an important part of a sediment budget, which is notoriously difficult to estimate.

Vertical accretion, the *slow* accumulation of overbank sediment without appreciable lateral channel migration, is the primary process by which most lowland floodplains develop (Nanson and Croke, 1992; Middlekoop and Van der Perk, 1998; Walling and He, 1998). Floodplains are known to be important locations for sediment storage in fluvial systems (Phillips, 1992a; Steiger et al., 2001; Noe and Hupp, 2009). Coastal Plain floodplains may be inundated multiple times a year, often for extended periods, particularly during the winter and spring (Hupp, 2000; Osterkamp and Hupp, 2010). Particulate storage in the Coastal Plain can be long (decades or much longer) with minimal erosion caused by lateral channel migration and little remobilization and export of floodplain sediments (Meade, 1982; Walling et al., 1996; Raymond and Bauer, 2001). Coastal Plain riverbanks may be low and inundation characteristically extends across the entire floodplain,

* Corresponding author. Tel.: +1 703 648 5207; fax: +1 703 648 5854.
E-mail address: crhupp@usgs.gov (C.R. Hupp).

significantly limiting flow competence. Natural levees, typically composed of sand, frequently form adjacent to the channel where relatively coarse suspended load sediments are deposited (Pizzuto, 1987; Hupp, 2000); these tend to be relatively high elevation floodplain features. Elevations become gradually lower away from the channel, passing through transition areas before reaching local topographic lows in broad backswamps. Elevations vary only a few meters (rare) or, typically, much less within the floodplain, and thus small differences in flood stage or groundwater elevation can substantially affect inundation frequency/duration across large areas and, thus, sediment deposition rates.

Most large Atlantic Coast rivers head in the Appalachian Mountains or adjacent Piedmont. Upon crossing the Fall Line and flowing on to the Coastal Plain, these sediment-laden rivers experience a dramatic regime shift (Hupp, 2000) from relatively high-energy, high-gradient systems to low-gradient meandering systems with broad, frequently and/or long inundated floodplains (Simmons, 1988). Research suggests that these floodplains may trap essentially all watershed derived sediment before reaching tide-dominated estuaries (Simmons, 1988; Phillips, 1992a,b, 1995, 1997; Kroes et al., 2007; Ensign et al., 2014).

Human alterations to the landscape and river system, such as flow regulation through dam construction (Grant et al., 2003; Nilsson et al., 2005; Knox, 2006) and land clearance with upland erosion and downstream aggradation (Trimble, 1974, 1983), have led to channel incision or filling and large changes in sediment supply conditions depending on the geomorphic setting (Schmidt and Wilcock, 2008). The downstream impacts from dam construction that most affect the floodplain are severe reductions in the peak stages, frequency, and duration of over bank flows, and sediment transport (Williams and Wolman, 1984). Land clearance with upland erosion, Piedmont channel erosion (Jackson et al., 2005), and downstream aggradation (legacy sedimentation dynamics; Costa, 1975; Jacobson and Coleman, 1986; Knox, 2006)

have led to channel and valley filling, and sometimes, subsequent channelization. These alterations may have heavily influenced the sediment dynamics of the lower Roanoke River (LRR), North Carolina, especially in terms of the connectivity of the floodplain to sediment-laden flood flow. Reductions in connectivity compromise the trapping function of floodplain ecosystem services, whereas anomalous connectivity increases may facilitate sedimentation (Hupp et al., 2008). Few models allow for prediction of the downstream effects of dams and even fewer that include the geological setting as a central factor. These deficiencies were addressed by Grant et al. (2003), who developed a model of channel change following dam construction that includes geology, climate, sediment supply, topography, and hydrologic regime; this was quantitatively extended in the development of physical metrics (drivers) to predict sediment balances below dams by Schmidt and Wilcock (2008).

The purpose of the present paper is to describe and interpret sediment deposition patterns, rates/amounts, and trends along the LRR between the upstream Piedmont dams and the Albemarle Sound estuary (Fig. 1). Specific objectives include (i) the interpretation of temporal and spatial sediment deposition patterns as they have varied in response to human alteration including legacy sedimentation and dam construction, (ii) interpretation of modern deposition patterns in relation to local elevation or hydroperiod and upstream/downstream trends, and (iii) the construction of a GIS-based flow-inundation/sedimentation model to improve sediment trapping estimations. The present paper is focused largely on temporal and spatial floodplain sediment deposition patterns. However, we also report and employ results from earlier and simultaneous studies on the LRR, including: an unpublished, until now, dendrogeomorphic analysis to obtain intermediate-term sediment deposition rates, a recent bank erosion study (Hupp et al., 2009a), pollen-based paleohydrologic studies

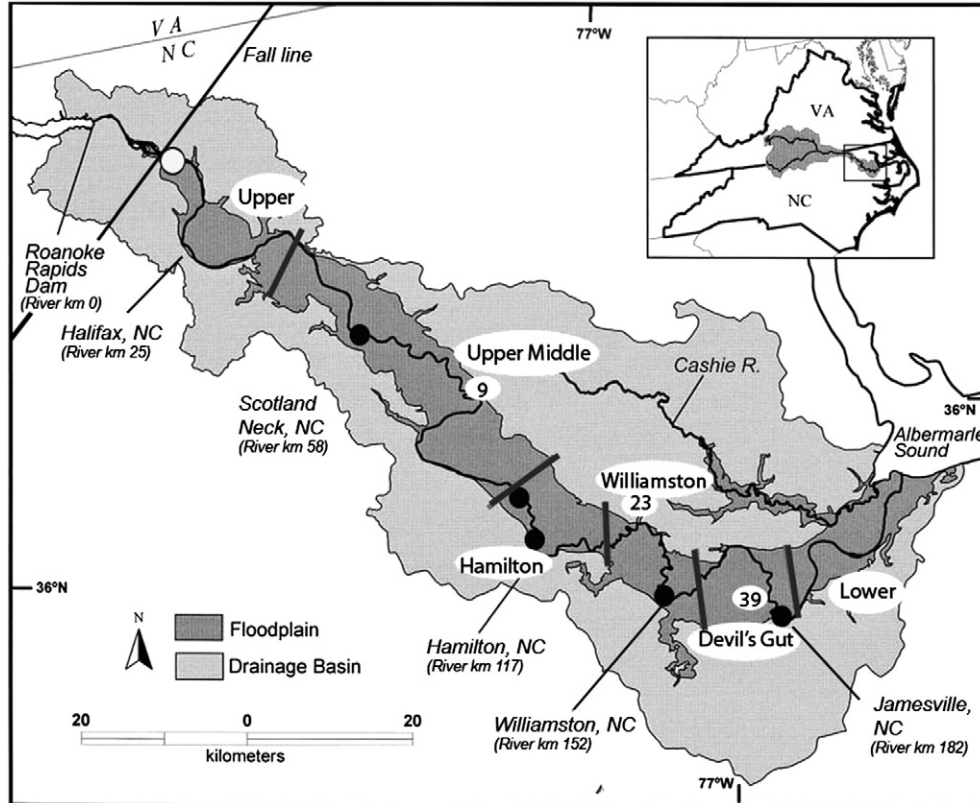


Fig. 1. The lower Roanoke River basin. Drainage basin below dams is indicated in light gray, floodplain areas are indicated in dark gray, main image is delineated into the six functional floodplain segments separated by heavy lines. The study area extends from the Fall Line to the Albemarle Sound. Approximate locations of transects 9, 23, and 39 are shown. The discharge gaging station (open circle) is located just below the dam in Roanoke Rapids; five other stage-only gages are located downstream and indicated by closed circles, most are associated with nearby towns, shown with river kilometer.

(Townsend et al., 2004; Willard, et al., 2010), and vegetation distribution/floodplain inundation/GIS studies by Townsend and Walsh (1998, 2001). This study was part of a larger effort funded in part by NSF grant EAR GEO 0105929, the USGS National Research Program, the USGS Climate and Land Use Change Research and Development Program, The Nature Conservancy, and the U.S. Fish and Wildlife Service.

2. Regional and site setting

The LRR is located on the northern Coastal Plain of North Carolina (southern part of the Mid-Atlantic Region), an area of broad upland plains with low relief and broad sometimes underfit bottomlands (Hupp, 2000). This region is characterized by humid temperate climatic conditions with a mean annual temperature of 15.8 °C and average annual precipitation of 1267 mm as measured at Williamston, NC, elev. 6.1 m (NGVD 1929) above sea level (station 319440 Williamston 1E, 1971–2000 Climate Normals, State Climate Office of North Carolina). The river flows generally east-southeast about 220 km from near the Fall Line to the Albemarle Sound as a largely single-threaded meandering stream (Fig. 1) across Miocene sedimentary material overlain by Quaternary Alluvium (Brown et al., 1972). The material consists largely of unconsolidated fine sands, silt, and clay, although the clayey Miocene deposits may be indurated. Additionally, the floodplain along the lower river trapped a large volume of sediment associated with post-colonial agriculture (Hupp, 1999). This sediment occurs along broad floodplains forming large distinctive levees (Hupp et al., 2009a). This legacy sediment (James, 2013) may be between 4 and 6 m in depth along upstream reaches of the lower river (P. Townsend, University of Wisconsin, written communication, 2006), which thins downstream to near zero close to the Albemarle Sound. Near surface floodplain soils are composed of red-brown fines (silt and clay, <63 μ) with considerable mica flakes, indicative of Piedmont origin and legacy processes (Phillips, 1992a,b). These soils are relatively organic rich and contain abundant *Ambrosia* (ragweed) pollen, indicative of deposition during and after colonial agricultural activity between about 150 and 250 years ago (Willard et al., 2010). The river is generally incised through the legacy sediment and other Coastal Plain sediments; although erosion on cut banks and many straight reaches appears active, point-bar development is limited. The floodplain along the LRR supports the largest contiguous Bottomland Hardwood forest on the Atlantic Coastal Plain (Hupp, 2000).

The modern LRR however descends from the Fall Line relatively sediment starved below three high dams (built on the Piedmont in the 1950s and 1960s, other dams exist upstream). The dams in the Piedmont were completed along the Roanoke River, North Carolina, between 1953 and 1963. The largest of these forms the John H. Kerr dam and reservoir (about 1.5 million acre feet storage), which controls major water discharges downstream and is currently under evaluation through a Federal Section 216 study (authorized review of operations) conducted by the U.S. Army Corps of Engineers for flood control effects. Two smaller hydroelectric dams located downstream of the Kerr Reservoir are the Gaston Dam that has operated as a power station since 1963 and farther downstream the smaller Roanoke Rapids dam that has operated as a power station since 1955; both of these dams are regulated by the Dominion Power Company (Dominion Virginia/North Carolina Power). The ecological effects of these dams were investigated by Richter et al. (1996) who developed a series of biologically relevant hydrologic attributes that characterize intra-annual variation in flow conditions and used the LRR as a case study. Flood-control operations on the Roanoke River have had large hydrologic impacts including the elimination of high-magnitude flooding and a greater frequency of high and particularly low flow pulses; this impact has been implicated in various forms of ecosystem degradation (Richter et al., 1996; Pearsall et al., 2005). Progressive channel and bank erosion downstream of the dams increase suspended sediment loads, which may then be deposited farther downstream. A sediment balance between sediment deposition and bank erosion on the Roanoke River (Hupp et al., 2009a) suggests

the lower floodplains still trap essentially all of the sediment eroded upstream on the LRR before reaching the Albemarle Sound (Fig. 1).

The average water discharge (1964–2007) is 228 m³/s as measured at Roanoke Rapids, North Carolina (USGS stream flow gage 02080500) below the downstream-most dam; daily mean discharges range from 23 to 1008 m³/s over the recent period of record (43 years). The gage has been operating since 1912 and was originally called the Roanoke River at Old Gaston. Prior to dam construction, annual peak flows regularly ranged from about 1400 to 2800 m³/s with extreme events in excess of 3400 m³/s (Fig. 2). Over the present gaging station record (since Kerr dam completion, 1953) the maximum peak flow was 1055 m³/s with normal peak-flow maxima about 980 m³/s. Conversely, low flows are sustained at higher discharges than before dam construction. Annual peak flows rarely are <220 m³/s, and most peaks are held around 560 m³/s (Fig. 2). Dominion Virginia Power controls hydroelectric generation at the downstream-most dam (Roanoke Rapids), which has direct bearing on short-term water stages along much of the lower river through peaking operations. Peaking operations (short-term rapid water releases to generate power) typically discharge about 500 m³/s for a short period increasing flows from ambient discharges that may be as low as 50 m³/s. Peaking may occur once or twice daily especially in the summer and fall and may have substantial impacts on inundation patterns over low parts of the floodplain (White and Peet, 2013). Water stage information is recorded at six stream flow gages along the lower river from Roanoke Rapids (also the discharge measurement station) near the dam and, in downstream order, stage only gages at Halifax, Scotland Neck, Hamilton, Williamston, and Jamesville, North Carolina, nearest the Albemarle Sound (Fig. 1).

3. Methods

Fifty-eight transects were selected to represent the downvalley trends in vegetative, hydrologic, and sedimentation patterns along fairly equally spaced locations (determined by GIS analysis of aerial photography) covering most of the Coastal Plain reach of the Roanoke River (about 210 km) from near the Piedmont dams to the Albemarle Sound (Fig. 1). Exact location (± 50 m) and orientation (± 3 – 5°) of transects was largely a random process, controlled by field-related exigencies at the time of placement. Transect selection was also constrained by property ownership and degree of intact mature vegetation. Sampling points along each transect were largely random, approximately equidistant, and stratified to assess major floodplain features including levees, backswamps, and transitional areas; a total of 378 stations were arrayed along the transects. Transects ranged in length from 100 to 2200 m with a minimum of 3 sampling stations and a typical maximum of 10 sampling stations, a few of the longest transects had up to 12 stations. All transects were surveyed to a temporary benchmark using a rod and optical or laser level (accuracy ± 2 mm/50 m).

These transects form the design and structure for the present study. They also are the sites for coring the floodplain deposits for pollen analyses and vegetation studies associated with the larger NSF-funded effort. To a lesser degree, they were used in the bank erosion studies (Hupp et al., 2009a) and the paleohydrologic study (Willard et al., 2010). The locations of earlier dendrogeomorphic efforts to measure deposition rates are intentionally overlapped by the present transects. Note, we use the term floodplain to apply to all features that are regularly flooded, including those that remain inundated for large parts of the year; the coastal situation of the river does not conform to some tenets of more traditional definitions of the floodplain (Osterkamp and Hupp, 1984).

3.1. Short-term clay pad analysis

Information from clay pads (feldspar markers) form the bulk of the results presented, used, and discussed in this paper. Artificial marker layers (clay pads) were placed at each sampling station. These markers

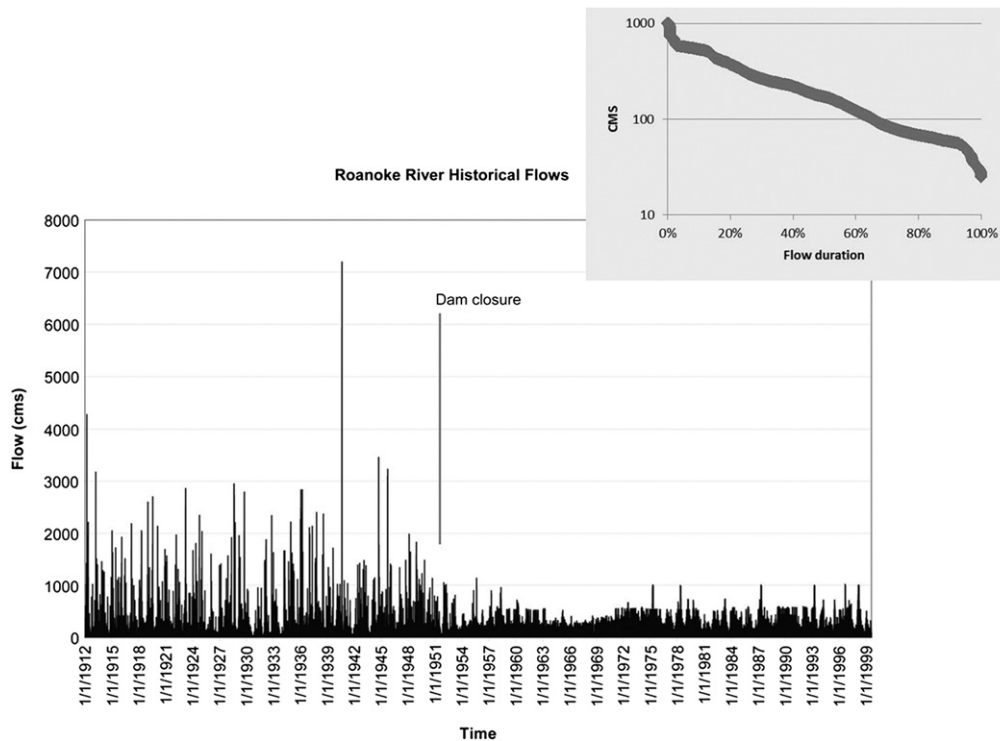


Fig. 2. Historic peak discharges (daily) on the lower Roanoke River since 1912 when the river was first gaged, present gage is at Roanoke Rapids (since 1964) and downstream from all dams. First dam closure (1953, Kerr Reservoir) is indicated. Inset: the regulated flow duration curve in cubic meters per second for the lower river.

are made by placing powdered white feldspar clay ~20 mm in thickness over an area of about 0.5 m² on the soil surface that has been cleared of coarse organic detritus. This clay becomes a fixed plastic marker after absorption of soil moisture that permits accurate measurement of short-term net vertical accretion (Bauman et al., 1984; Hupp and Bazemore, 1993; Kleiss, 1996; Ross et al., 2004). The clay pads (378, one at each station) were established in 2001 and 2002 and then examined and measured for depth of burial to estimate net fine-grained deposition over a 3-year period from 2003 through 2005. All pads were measured two to five times during this period depending on access, which was limited by inundation. All burial depths were converted to a net annual rate of deposition. A subset of 24 transects were remeasured in 2010 with an additional three transects measured in 2012 after 8 and 10 years of deployment, respectively. The two recent measurements, although incomplete, allow for significantly longer term estimation from clay pads than is typically reported. The comparison of deposition amounts over this time interval may better account for compaction and organic-component losses.

We calculated net deposition as the mean of at least three measurements to the nearest millimeter for each pad during each sampling interval. Coarse organic material (stems and leaves) are not included in net deposition amounts. Each clay pad is identified as being located on either a levee, transition, or backswamp surface; whole transect averages of net deposition include all floodplain clay pads. Sediment samples were taken near all clay pads to a depth of 20 mm and analyzed for (i) bulk density, by taking a known sample volume, which was then dried and weighed; (ii) size clast composition by dry sieving with various screen sizes in a vibratory sieve shaker (Guy, 1969); and (iii) organic fraction of the sample by loss-on-ignition (400 °C for 16 h; Nelson and Sommers, 1996). Using bulk density information, rate data were converted to mass and reported as grams per year, which provides standardized and more easily comparable inter-site results; both rate and mass values are presented. Results from the clay pad analyses were compared to those from dendrogeomorphic and core pollen analyses. Clay pad analyses provide present day deposition

rates that may be compared to dendrogeomorphic rates that more fully encompass the period since dam construction and to pollen analyses that encompass legacy sedimentation processes.

3.2. Intermediate-term dendrogeomorphic analysis

Dendrogeomorphic techniques provide a net rate of floodplain sediment deposition over the life span of any sampled individual tree (typically decades to centuries). We conducted dendrogeomorphic analyses in two time periods. First, in 1997–1998 on 16 transects (located near those described above) at nine sites along the river that overlap with the main NSF study. Ten to 65 trees were sampled along each transect (usually about 40 depending on species availability and intra-station distances); a total of 462 trees were sampled for floodplain deposition rates. A second dendrogeomorphic sampling effort occurred during the main NSF study (2002–2005) along 10 of the transects (described above); 203 additional trees were sampled in this effort. Sampling several trees at stops along a transect is necessary to account for local depositional variation and to ensure the determination of a mean rate with an acceptable standard error (SE < mean). At least 10 trees were sampled at specific stations, usually stratified by landform, on the transects. The procedure follows that of Sigafos (1964) where the specimen trees are partly excavated down to the top of the normally horizontally radiating root mass, a level that is established at the time of germination; detail for this procedure including sampling design is described in Hupp and Bornette (2003). We measured the depth of burial from the top of major roots to the present ground surface to provide a conservative estimate of net sediment deposition during the life of the tree. The tree is then cored near its base with an increment borer; the extracted core is returned to the laboratory for cross-dating and age determination. The depth of burial above the root collar is divided by the age of the tree to provide an estimate of net deposition rate. Depth to roots was measured at a distance away from the trunk that was approximately equal to the trunk diameter at ground surface to avoid the collar curvature. This technique has been shown to be

internally consistent and has been used with considerable success along streams in the southeastern USA (Hupp and Bazemore, 1993; Hupp et al., 1993; Ross et al., 2004; Jolley et al., 2010), the Great Plains regions of the United States (Friedman et al., 1996; Scott et al., 1997; Heimann and Roell, 2000), and in France along the Ain River, a tributary to the Rhône River (Piégay et al., 2008). We preferentially sampled certain species because they were common at the sampling stations, have easily determined ring boundaries, do not experience multiple and/or missing rings to the degree of other species, and they have a well-developed collar curvature with horizontal roots near the trunk. These species include *Fraxinus pennsylvanica*, *Celtis laevigata*, *Ulmus americana*, *Platanus occidentalis*, and a few oak species, *Quercus*. We also occasionally sampled *Nyssa aquatica/biflora* and *Taxodium distichum* in wet backswamps; the former suffers from difficult ring-boundary determination and the latter from buttressing and sometimes ambiguous major root development. Deposition rates from these trees may be less accurate than those from the more frequently sampled species.

3.3. Pollen analyses from soil cores

Sediments deposited after Colonial land clearance in eastern North America are characterized by common (>2%) *Ambrosia* (ragweed) pollen. *Ambrosia* is an early succession plant that occupies sites within a year of clearance (Bazzaz, 1974; Keever, 1983), and previous studies have shown sharp increases in *Ambrosia* pollen after early Colonial land clearance began (Brush, 1984; Willard et al., 2003). We used common ($\geq 2\%$) occurrence of *Ambrosia* pollen to identify floodplain sediments deposited after ~A.D. 1700.

Fifty-seven sediment cores were collected for pollen analyses on 29 transects from the Fall Line to Albemarle Sound. The cores were located on the levee, backswamp, and intermediate sites. Pollen was isolated from the surface and basal samples of each core, as well as from lithologic changes, to identify coarse-scale changes in pollen assemblages throughout the history of the site. Approximately 3–10 g of dry sediment was used for palynological analysis, depending on lithology. After drying and weighing samples, one *Lycopodium* marker tablet was added to each dried sample for eventual calculation of absolute pollen concentrations (Stockmarr, 1971). Samples were demineralized using HCl and HF before being acetolyzed (nine parts acetic anhydride:one part sulfuric acid) in a hot-water bath (100 °C) for 10 min. After neutralization, they were treated with 10% KOH in a hot-water bath for 15 min. Neutralized samples were sieved with 10 and 200 μm sieves, and the 10–200 μm fraction was stained with Bismarck brown, mixed with warm glycerin jelly, and mounted on microscope slides. Raw data and metadata for pollen samples are deposited in the North American Pollen Database (NAPD) at the World Data Center for Paleoclimatology in Boulder, CO, USA (<http://www.ncdc.noaa.gov/paleo/napd.html>). Pollen and spore identification (minimally 300 grains per sample) was based on reference collections of the U.S. Geological Survey (Reston, Virginia).

3.4. Hydrogeomorphic and GIS analyses

The lower river has been divided into various segments in previous studies (Townsend and Walsh, 2001; Hupp et al., 2009a; Moulin et al., 2011) based on units derived from arbitrary river lengths to statistical similarity analyses. Although we use some arbitrary segmentation in reporting earlier studies, the present paper breaks the river into six segments (Fig. 1) delineated hydrogeomorphically using functional floodplain area, bank height, and position of the channel relative to the downvalley axis as key elements. The functional floodplain area is defined by the Townsend and Walsh (2001) numerical model as modified by White and Peet (2013) and refers to parts of the floodplain that are usually flooded one or more times per year with varying duration. The functional floodplain can then be systematically categorized into GIS grid units

representing flooding along an inundation gradient (calculated for each river segment); we separated these units (polygons, irregular) into 12 coded categories, or grid units. The polygons have a spatial resolution of 3 m. Grid code units 2 through 13 represent decreasing inundation periods as determined by the hydrologic model for the floodplain as adjusted by White and Peet (2013) who used extensive in situ well data to correct inundation periods. Each unit beginning with 2 (inundated at discharges between 84 and 168 m^3/s) increases by 84 m^3/s with a spread of 84 m^3/s for each ascending unit, such that unit 3 is inundated at discharges between 168 and 255 m^3/s and so forth through to unit 13, which includes all discharges greater than 1008 m^3/s . The units are mapped in each of the river segments and attributed with deposition rates determined from clay pads in that unit so that deposition can be converted to mass (Mg/y) using segment specific bulk density and areal extent of the unit.

Mean sediment deposition rates are assigned to each of the GIS grid units from data obtained over co-located individual clay pads. The area of each grid unit was then determined for each of the six river segments. This breakdown allows for more representative determination of sedimentation patterns from upstream to downstream parts of the floodplain and along geomorphic gradients (e.g., levees versus backswamps). Further, we analyzed deposition patterns for organic and mineral components of the sediment and related these to inundation categories (grid unit). The Roanoke River floodplain is classically underfit (Hupp, 2000) with large areas of floodplain that are periodically inundated but do not receive sediment-laden water. To correct for possible over estimation of deposition we used a 1.2 km buffer, so that parts of the bottomland more distant from stream flow could be excluded from analyses. Results from this and our previous studies showed that river-derived deposition in deep backswamps far from the river (poor connectivity) was low to nonexistent; this distance using long transect information is about 1.2 km. Nonfluvial deposition, from autochthonous organic duff and potential aeolian sources is estimated from deposition on levee pads that were not flooded during the major study period (2002 through 2005). We measured an average 1.3 mm/y over these noninundated clay pads, which compares to the 1.7 mm/y on nonflooded clay pads on the highly productive, relatively open floodplain along the Kissimmee River, FL (Schenk et al., 2012). The nonfluvial rate (1.3 mm/y) was subtracted from overall rates prior to conversion of rate to mass estimates calculated for determining floodplain sediment trapping throughout the study area; these corrected rates are termed *net rates* henceforth.

4. Results

These results are derived from up to 10 years of clay pad sediment depth measurements and two separate, though reasonably co-located, dendrogeomorphic analyses completed in 1999 and 2006, respectively; a total of 665 trees were sampled. The following floodplain sediment deposition information is presented to show downvalley trends in sedimentation patterns at the scale of the six river segments and to show local or landform/elevation variation. These trends are contrasted by providing information from the relatively conservative deposition estimates using dendrogeomorphic techniques (Hupp and Bornette, 2003) and from the artificial marker horizon estimates (clay pad) that potentially overestimate deposition rates (Craft, 2007; Noe and Hupp, 2009). Most comparative results are shown in deposition rates (mm/y) for ease of interpretation and because most of the dendrogeomorphic sampling design was not developed to construct mass (Mg/y) estimates. The floodplain sediment accumulation estimates use only information from the complete clay pad analyses (2003 through 2005) and are reported in terms of mass. Temporal variation in floodplain sediment deposition is presented using dendrogeomorphic estimates from age cohorts and by type of analyses: clay pads – short term, dendrogeomorphic – intermediate term, and pollen – long term.

4.1. Spatial trends in sedimentation patterns

Mean deposition rates as determined from dendrogeomorphic analyses, considering all landforms, ranged from 0.5 to 3.4 mm/y; rates determined from clay pads (net) were generally higher and ranged from 0.3 to 5.9 mm/y (Table 1). Dendrogeomorphic evidence indicates that sedimentation rates are lowest in the upstream-most reaches and systematically increase to the Devils Gut segment where they are the highest (Fig. 3); rates decrease in the lower-most segment. This same pattern is generally true for clay pad derived sedimentation rates (Fig. 3), especially when considering deposition in backswamps where the highest clay pad rates occur (Fig. 4). The dendrogeomorphic analysis (Table 1) and the uncorrected, raw clay pad estimates (not shown) display a distinct drop in deposition rate at the Williamston segment. This segment is dominated by an extensive levee and levee/transition area, which is now inundated infrequently because of flow regulation.

Mean levee deposition rates are generally lower (1.6 mm/y) than mean backswamp rates (2.5 mm/y) from dendrogeomorphic data (Table 1). This is also true for the more recent short-term clay pad data, where levees averaged 1.5 versus 3.7 mm/y for backswamps (short-term rates are net rates that have been adjusted by a correction factor to account for nonfluvial deposition, explained previously). The clay pad analyses separated the landforms into three categories (Fig. 4) based on floodplain inundation categories (explained subsequently) by delineating a transition zone between the hydrologically and vegetatively distinct levees and backswamps. The mean clay pad deposition rate for transition areas was 1.6 mm/y, slightly higher than levee deposition, and is heavily influenced by the Devil's Gut rate (Fig. 4).

Three transects were selected to show detailed deposition patterns relative to elevation from the Upper Middle, Williamston, and Devils Gut segments, transects 9, 23, and 39, respectively (Figs. 1 and 5); deposition rates are from clay pad analyses. Transect 9 crosses a neck such that levees occur at both ends (levee at start is the upstream side of neck), whereas transects 23 and 39 extend from the levee and end in the backswamp. In order from upstream, they have raw mean clay pad deposition rates of 2.5, 5.5, and 10.1 mm/y, respectively, clearly substantiating the trend for increasing deposition rates from upstream to the Devils Gut Segment. Further, two typical trends along transect (local) are exposed. Deposition rates are usually highest in low, backswamp, and transitional parts of the transects, which is true for most river segments (Fig. 4) and low on levees. The peak on transect 23 is associated with an active slough (obvious from level line, Fig. 5)

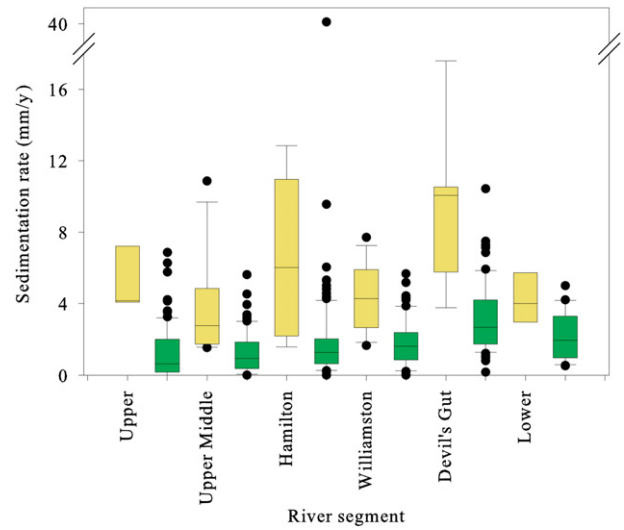


Fig. 3. Box plot results of sedimentation rates at the six river segments; tan boxes are from raw clay pad analysis and green boxes are from the combined dendrogeomorphic analyses and are consistently lower than the clay pad rate. Box encloses 25 to 75%, whiskers include 10 and 90% of results; line indicates the median and points are outliers.

that conveys sediment laden river water and maintains a relatively high connectivity. Deposition rates tend to ultimately diminish with distance from the channel approaching the low rates typically associated with levees (Fig. 5); the peak at the end of transect 9 occurs because the last clay pad was established on a point bar, not the levee.

4.2. Temporal sedimentation trends

Age cohort analyses from dendrogeomorphic study have been used with some success to infer changing deposition rates through time (Hupp and Bazemore, 1993; Heimann and Roell, 2000). We used the dendrogeomorphic analyses to investigate temporal variation by separating the samples into cohorts by four age classes: 0–29, 30–59, 60–99, and 100–150 years old at year 2005 (same year as most final clay pad readings). No distinct trends in the upper three segments occur either along the river or by age class (Fig. 6). The two oldest age classes, 60–99 and 100–150 years demonstrated only a slight increase in deposition rates in the lower three segments (Fig. 6). Whereas the

Table 1

Summary of mean sedimentation rates, by segment, from dendrogeomorphic evidence (combined data) and clay pad analyses (net/corrected values), depth to colonial agricultural horizon from pollen analysis, and selected parameters for sedimentation modeling using GPS grid code techniques.

River segment	Upper	Upper Middle	Hamilton	Williamston	Devil's Gut	Lower	Means
Dendro-NSF, mm/y	0.7	1.7	1.9	0.6	2.7	0.5	1.4
Dendro-pre NSF, mm/y	1.2	1.3	1.8	1.9	3.4	2.3	2.0
Levee	1.2	1.3	1.8	1.8	2		1.6
Backswamp		1.3	2.1	2.9	3.9	2.3	2.5
Claypads, mm/y	2.2	1.6	2.8	3.5	5.3	0.9	
Levee	2.7	1.1	0.3	1.6			1.5
Transition	0.4	0.4	1.1	1.6	5.9	0.4	1.6
Backswamp	1.9	3.2	3.9	5.0	5.6	2.8	3.7
Pollen cores,							
Depth to Ag. horizon (m)							
Levee	5.00	3.75	2.68	3.24	0.97	0.38	2.67
Transition	1.65	1.19	1.13	0.75	0.91		1.13
Backswamp		0.91	1.00	0.95	0.57		0.86
Sediment modeling							
Bank heights (mean, m)	5.1	5.0	3.7	2.4	0.9	n/a	
% Grid code 6 or wetter	40	55	79	83	86	91	
% in backswamp	27	34	48	58	77	84	
Bulk density (g/cm ³)	0.63	0.60	0.55	0.52	0.46	0.43	
% loss on ignition (LOI)	15	16	17	17	17	20	

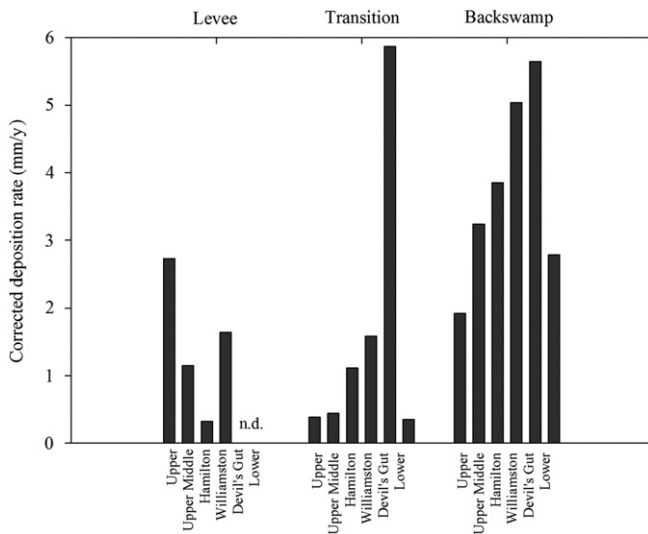


Fig. 4. Clay pad net deposition rates by river segment and landform. The peak at the Devils Gut transition zone is anomalous and results from the lack of a levee in a high depositional area such that a transition elevation is the first site for overbank deposition. The backswamp traps the most sediment in general and in all segments except the Upper. No data (n.d.) is indicated for sedimentation rates on levees at the two lowermost segments where levees do not generally form.

most recent age classes, 0–29 (especially) and 30–59 indicate a distinct increase in deposition in the lower three segments peaking at Devils Gut (Fig. 6); this period is coincidental with the period since dam closure. Note that deposition estimation for old age classes is complicated by the potential muting effects of subsequent deposition; although this cohort analysis may be a blunt, imprecise estimate, it remains the best, easily interpretable form of reporting relative temporal trends from dendrogeomorphic data (Hupp and Bazemore, 1993).

Pollen analyses to measure deposition since European settlement documents considerable deposition along the river. The agricultural horizon, as marked by increased abundance of *Ambrosia* pollen, is at least 5 m below present ground surface at levee sites in the Upper segment and diminishes to less than a meter at levees in the Devil's Gut segment (Table 1). Locally, this legacy deposit is much less substantial in some transition and all backswamp parts of the floodplain than in levees. The legacy deposition period began approximately between A.D. 1700 and 1750; we use 1725 as a general start date for the onset of the floodplain deposit. The oldest tree cohort extends back about 150 years before A.D. 2000, thus back to about 1850. Given that we see little evidence of substantial deposition in this oldest age cohort in any segment (Fig. 6), we assume the legacy deposition period ended prior to about 1850, providing for a 125-year period. Using this 125-year period, levee deposition rates on the reach including the Upper and Williamston segments are estimated to have ranged between 23 and 40 mm/y, an order of magnitude greater than present day rates estimated from clay pads (Fig. 7). However, 8 to 5 mm/y legacy rates at the Devil's Gut and Lower segments are quite similar to modern clay pad estimated rates (Fig. 7). Note that legacy deposition thickness includes modern deposits (since 1850 and dam closure).

4.3. Floodplain sedimentation modeling

Estimation of present floodplain sedimentation patterns and trends using a GIS model was facilitated by the separation of the floodplain into six segments (Fig. 1) based on functional floodplain area and various geomorphic characteristics, as described earlier. Each segment was further divided into three relatively distinct geomorphic features, namely levee, transition, and backswamp. The Upper segment has distinctively high banks (Table 1, in some locations >6 m high), a small functional floodplain that is relatively narrow in relation to downstream

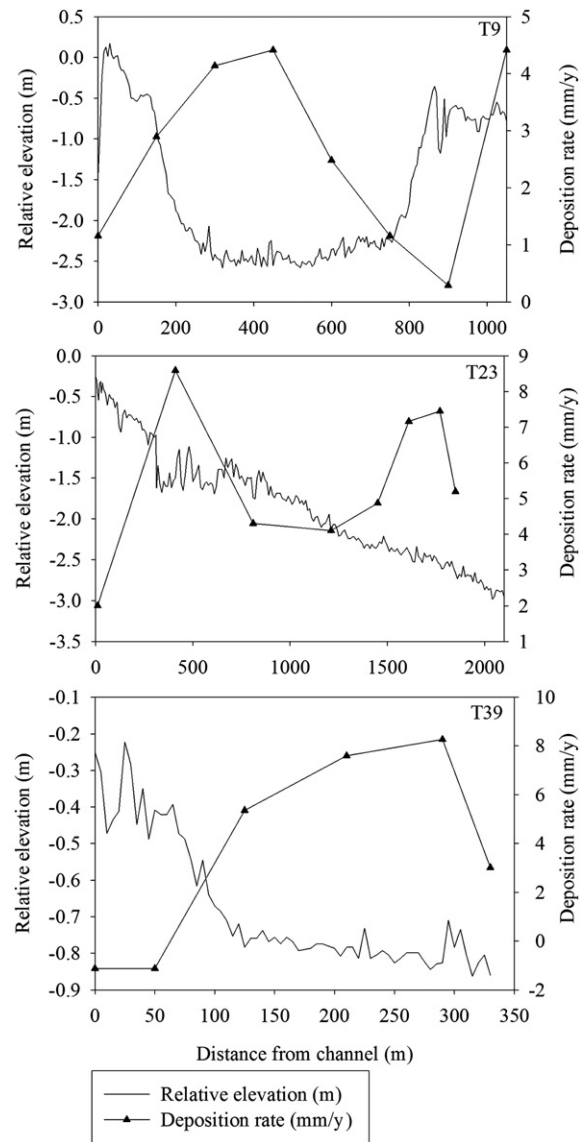


Fig. 5. Transect elevation (solid line) and clay pad sedimentation rates (triangle symbols with connecting lines) for three transects selected to generalize patterns seen along the LRR; T9, T23, and T39 are located in upstream to downstream order in the Upper Middle, Williamston, and Devil's Gut segments. Note that T9 crosses a neck in the river such that it begins and ends on a levee. The sedimentation peak at the end of T9 reflects its location on a point bar and not typical of levee deposition. The peak near the beginning of T23 is associated with an interior slough that carries sediment-laden water during high flow and increases connectivity between stream flow and the floodplain.

segments, and is inundated a small amount of time (short hydroperiod, length of time annually when inundation occurs). The Upper Middle segment is large in floodplain area and areas with hydroperiods that are influenced by even moderate flows; bank heights are similar to the Upper segment (Table 1) and remain distinctively high relative to downstream segments. Fluvial erosion (particle-by-particle) is greatest along this segment although the banks have less mass wasting (bank failure) than segments immediately downstream (Hupp et al., 2009a; Moulin et al., 2011). The Hamilton segment is characterized by a broad functional floodplain with extensive backswamps. This segment has the highest rate of mass wasting on banks that are moderately high (Hupp et al., 2009a). The Williamston segment is similar to the just upstream Hamilton segment, has somewhat lower bank heights, but is distinguished by long transverse reaches that extend from one side of the active valley to the other (Fig. 1). This orientation of the channel to the downvalley axis facilitated the development of distinctive,

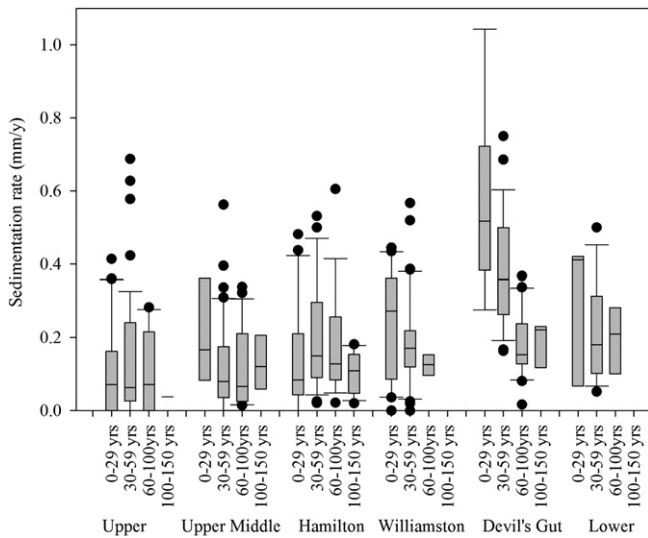


Fig. 6. Box plots of sedimentation rates determined from dendrogeomorphic evidence by age cohort and river segment. Note that the oldest cohort, 100–150 years old, show no elevated rates, suggesting that legacy deposition likely occurred prior to 150 years ago. Box encloses 25 to 75%, whiskers include 10 and 90% of results; line indicates the median and points are outliers.

particularly wide levees and transitional areas on the downvalley side of these reaches (Fig. 8), presumably, mostly formed during the legacy aggradation period. Conversely, large interior sections of the floodplain consist of backswamps that persist to nearly the upvalley side of the downstream channel bend (Fig. 8). Below Williamston along the Devil's Gut segment a relatively abrupt reduction in bank height (most banks 1 m or less high) and levee area occurs. This segment contains a large functional floodplain that is partly inundated at even moderately low flows; most of this floodplain is in backswamp and supports an extensive bald cypress–tupelo gum forest. The Lower segment, nearest the Albemarle Sound, is generally similar to the Devil's Gut Segment except banks are essentially nonexistent and only small amounts of levee/transition features sporadically occur. Parts of the floodplain are nearly continuously flooded and all of the floodplain is subject to complete inundation from wind tides.

Basic statistics and results of the GIS model grid code calculations for the entire river floodplain are presented in Table 2. Sediment deposition rates in terms of mass (Mg/y) for mean and median values for each grid-code unit generally decrease from low to high discharges necessary to inundate surfaces within a particular grid code (long to short hydroperiods). Most of the floodplain has relatively long hydroperiods,

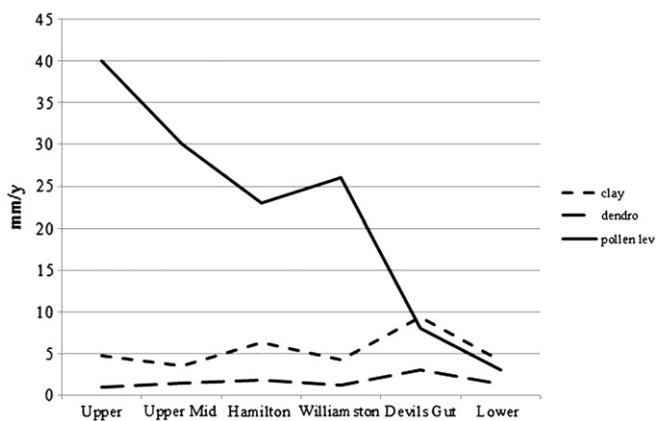


Fig. 7. Comparison of the three measurements of sediment deposition rates across three time scales by river segment; short-term or annual by clay pad analysis (net), intermediate-term or decadal by dendrogeomorphic analysis, and long-term or pollen analysis.

74% of the functional floodplain is within grid code range of 2–6 (Table 2). Thus, nearly three-quarters of the floodplain is inundated by median discharges (420–504 m³/s). Inundation of this part of the floodplain occurs between 12 and 16% of the time annually; based on the flow duration curve (Fig. 2) developed from gaging station records for the 50-year period (1960–2010) since dam operations. Further, 84% of the annual mass of median sediment deposited is within the 2–6 grid code range (Table 2).

The grid-code unit deposition rate when multiplied by the amount of each code in a segment and summed provides an elevation/hydroperiod net estimate of total mass per year of sediment trapped within a given segment; these are shown in Table 3. These estimates have been further adjusted by the 1.3 mm/y reduction in sedimentation rate to account for nonfluvial deposition (predominantly organic) and buffered so that floodplain areas farther than 1.2 km from the river are not included. This buffer was determined from clay pad analyses that show most suspended sediment has been removed after a traverse of this distance across the vegetated rough floodplain surface. These trapping estimates are calculated using bulk densities that are adjusted for landform (levee, transition, backswamp) and segment; mean bulk density ranges (Table 1) from a high (0.63 g/cm³) at the upstream-most site and a low (0.43 g/cm³) at the downstream-most site. Approximately 453,000 Mg of sediment is presently trapped on the LRR floodplain per year. Trapping rates are generally variable over a short range (about 2000 Mg/y) for the four upstream segments (Fig. 9); trapping was highest in the Devil's Gut segment with a rapid decrease to the lowest trapping rates at the Lower segment. Mineral deposition, which constitutes between 80 and 85% of total deposition (Table 1), mirrors total deposition patterns. The organic fraction trapped is small and shows little variation throughout the river except for an increase at Devil's Gut (Fig. 9).

5. Discussion

The floodplain of the LRR has been heavily impacted by human alterations since the early 1700s by severe aggradation associated with post-colonial agriculture and culminating with high dam construction (3) in the 1950s along the main stem in the Piedmont. These dams had a collective estimated trapping efficiency of 95%, effectively preventing most of the 87.5 Mg/km²/y (sediment yield at Fall Line) from passing into the LRR (Simmons, 1988). A few geographic qualities on the LRR allow for detailed identification of the basin-scale processes responsible for sediment deposition patterns. Namely, no significant tributaries exist between the dams and the Albemarle Sound (Fig. 1), which allows for a close look at downvalley processes that might be obscured by tributary confluences. Further, the watershed area below the dams is greatly restricted relative to upstream, which limits the potential input of upland erosion along the LRR. Thus, nearly all sediment presently in transport and deposited on the floodplain must come from the channel bed and banks. Additionally, given that the bed of the river is predominantly sand except along the lowermost reaches (from bathymetric surveys by the authors) and given that floodplain deposits since dam closure are silt/clays and largely devoid of sand, it can be argued that most current deposition is derived from banks. The legacy deposits (sediment sources) and regulated discharges from dams affect most aspects of present fluvial sedimentation dynamics along the lower river. The dominance of human alterations in affecting sedimentation patterns and processes is strongly supported in the literature (Phillips, 1995; Craft and Casey, 2000; Hupp et al., 2009b; Heath and Plater, 2010; Willard et al., 2010). Note that our estimation of the end of the legacy sedimentation period at about 1850 coincides with the cessation of The Little Ice Age (LIA) in North America, which represents a change in climate. This coincidence may have some bearing on our timing estimates but has not been specifically tested. We believe the agricultural practices distinctly outweigh possible sedimentation impacts associated with an LIA change in climate.

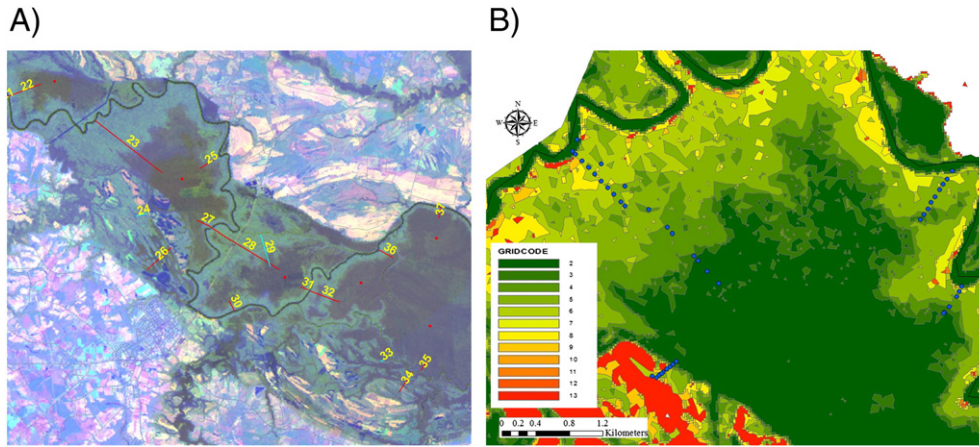


Fig. 8. (A) Aerial image of the Williamston and part of the Devil's Gut segments showing transect locations (yellow numbers) and approximate length (red lines). Note the greater development of levees (light shade) on the downvalley side of the main channel (e.g., transect 23) than the upvalley side of the main channel (e.g., transect 27). Dark shaded floodplain area is largely backswamp areas. (B) Detail of floodplain near transects 23 (left) and 25 (right) showing distribution of grid code units. Levee and high elevation areas are shown in light green to red, transition areas in intermediate green, and backswamp in dark green.

5.1. Comparison of analyses and impacts of human alteration

Few studies have directly compared feldspar marker and dendrogeomorphic determined rates of floodplain sedimentation (Hupp and Bazemore, 1993; Heimann and Roell, 2000); to our knowledge, this is the first study also to include comparison of long-term sedimentation rates derived from pollen analyses. Together, pollen stratigraphy results (Willard et al., 2010) encompassing the period from the early 1700s to near present (time of coring), dendrogeomorphic results encompassing the period from about 1850 to near present (about 2005), and clay pad results from 2001 to near present (2005–2012) provide comparative temporal information. Others have compared feldspar marker analyses to various isotopic radiometric analyses including ^{137}Cs and ^{210}Pb (Craft and Casey, 2000; Craft, 2007; Kroes and Hupp, 2010). Soil compaction, organic material decay, and other factors affect accumulation rates over time (Hupp et al., 2008) such that short-term techniques may overestimate long-term rates. We found a significant ($n = 149$, $p < 0.001$) 47% decrease in deposition rates calculated over the same clay pads on 24 transects when measured in 2005 versus 2010–12. However, 2003, the first full year after complete deployment of clay pads, was exceptionally wet with much of the floodplain inundated for most of the year. This wet year likely influenced the relatively high deposition rates for the three-year period ending in 2005. As previously noted above, short-term deposition rates from clay pad analyses tend to overestimate accretion (Heimann and Roell, 2000; Craft, 2007), which has been attributed to a lack of compaction and respiration of

organic material. Conversely, intermediate-term sedimentation rates estimated from dendrogeomorphic analyses may underestimate sedimentation, which is intentionally conservative through the design of the methodology (Hupp and Bornette, 2003). Our net sedimentation rates generally lie between these two boundaries (Fig. 10) and support our belief that the net rates are among the most accurate in the literature. Field measurement error may occur for clay pad and dendrogeomorphic techniques; using repeat measurements among several observers, error ranged between ± 1 and 1.5 mm (written communication by authors and A. Gellis, 2014). Pre-historic rates of sedimentation were most likely distinctly lower than the rates we report in response to human alteration. We estimate they ranged between about 0.4 to 1.0 mm/y depending on local situation; the lower estimate is based on deep soil core and radiocarbon information, while the higher estimate is based on a dendrogeomorphic analysis of old trees along stable reaches in the LRR. Because the time of rapidly changing land use practices (eighteenth century) is at the upper limit of confident radiocarbon dating, our dating of this horizon depends on a combination of historical accounts of land clearance and radiocarbon dates.

Our sedimentation rate estimates (both clay pad and dendrogeomorphic) compare similarly to most previously studied systems (Hupp, 2000; Aust et al., 2012) with a range of mean rates from 0.4 to 5.9 mm/y (Table 1). Aust et al. (2012) summarized sediment accretion rates in a variety of bottomland and riparian forests in the southeastern US and showed that although sedimentation rates vary widely, most are <10 mm/y, but range from 0 to over 500 mm/y in some

Table 2
Summary of sedimentation estimates by grid code, Dep rate refers to rate of sediment deposition.

Grid code unit	Discharge (m ³ /s)	Mean (mm/y)	Stdev	Median (mm/y)	Area (km ²)	Mean		Median	
						Dep rate (m ³ /y)	Dep rate (Mg/y)	Dep rate (m ³ /y)	Dep rate (Mg/y)
1	0–84								
2	85–168	8.96	10.38	6.28	128	1,143,296	624,058	801,623	437,559
3	169–252	5.48	4.06	5.33	41	224,680	122,640	218,590	119,315
4	253–336	7.79	8.38	4.47	44	342,760	187,093	196,842	107,445
5	337–420	5.12	6.43	3.16	50	256,000	139,735	157,760	86,112
6	421–504	3.73	3.68	2.16	32	119,360	65,152	69,167	37,754
7	505–588	2.81	2.65	1.63	12	33,720	18,406	19,571	10,683
8	589–672	3.06	4.43	1.43	11	33,660	18,373	15,713	8577
9	673–756	4.5	6.35	2.38	9	39,150	21,370	20,713	11,306
10	757–840	2.38	1.44	2.36	10	22,848	12,471	22,680	12,379
11	841–924	2.85	1.75	4.42	8	23,085	12,601	35,782	19,531
12	925–1008	4.94	5.47	2.32	13	64,220	35,054	30,127	16,445
13	>1008	3.67	4.11	2.87	43	157,810	86,139	123,388	67,350

Table 3

Sedimentation mean estimates by river segment showing net and buffered values for total, mineral, and organic components; amounts have been corrected for autochthonous nonfluvial deposition, yielding net sediment deposition.

	Sediment volume		Total sedimentation		Mineral sedimentation		Organic sedimentation	
	No buffer	Buffer	No buffer	Buffer	No buffer	Buffer	No buffer	Buffer
	m ³ /y	m ³ /y	Mg/y	Mg/y	Mg/y	Mg/y	Mg/y	Mg/y
Upper	92,762	92,762	58,642	58,642	50,100	50,100	8542	8542
Upper Mid	222,593	130,733	134,351	78,907	112,552	66,104	21,800	12,803
Hamilton	210,354	116,090	115,602	63,799	96,288	53,139	19,315	10,659
Williamston	281,386	152,374	145,149	78,600	120,564	65,287	24,585	13,313
Devil's Gut	434,452	296,120	197,916	134,899	164,575	112,173	33,341	22,725
Lower	52,487	88,632	22,578	38,127	18,069	30,513	4509	7614
Total	1,294,033	876,711	674,239	452,973	562,148	377,316	112,091	75,657

Louisiana bottomlands. Hupp et al. (2008) reported high sedimentation rates (at least 42 mm/y) also in Louisiana as part of a prograding deltaic process that deposits sediment in a wave-like fashion that peaks and subsides with the passing depositional front. We estimated a maximum of 40 mm/y, using a pollen tracer, during the aggradation associated with post-colonial agriculture in the Piedmont (Fig. 7) in the upper reaches of the LRR. The waves of legacy sedimentation occurring after the onslaught of colonial land clearance and agriculture along many streams in the eastern U.S. (Trimble, 1974; Costa, 1975; Jacobson and Coleman, 1986) may be analogous to the prograding deltaic depositional processes (Fisk, 1952; Tye and Coleman, 1989; Hupp et al., 2008) associated with the Mississippi and Atchafalaya rivers in Louisiana.

The bulk of the legacy deposition on the LRR is locally stored in levees and some transition areas (Fig. 5) particularly where the channel orientation is nearly normal to the downvalley direction, a feature exemplified in the Williamston segment (Fig. 8). Note also that the levee on the downvalley side of the reach is an order of magnitude more extensive than the levee on the opposite, upvalley side of the reach. This disparity likely occurs as a result of most of the suspended sediment being concentrated in the vicinity of the thalweg/channel during high flows until the flood stages attain and exceed the bank elevations. The sediment-laden water then has a flow orientation more in line with the valley (typically less sinuous) axis such that the downvalley levee/floodplain intercepts and filters out much of the suspended sediment before the flow reaches the more distant backswamps (Figs. 5 and 8). These large levee features can be seen in similar situations in aerial photography of many southeastern Coastal Plain rivers including the

Atchafalaya River (Hupp et al., 2008), although it is rarely (if at all) mentioned in the literature.

The dendrogeomorphic cohort-determined rates of sedimentation through selected time periods (Fig. 6) suggest that the levee-building episode on the LRR ended by about 1850, certainly prior to dam closure in the mid-1950s. Sediment deposition rates on levees since dam closure (dendrogeomorphic analysis) and present rates (clay pad analysis) are lowest on levees (near 0 at many sites) compared to transition and backswamp surfaces (Fig. 4) and strongly suggest that regulated flows are not competent to suspend sand sufficiently to provide levee deposition (Hupp et al., 2009a). However, additional hydrologic impacts from the dams also include sustained relatively low to moderate discharges that may inundate and deliver sediment to LRR backswamp areas for periods longer than prior to regulation (Richter et al., 1996; Pearsall et al., 2005). Together, reduced levee sedimentation with increased deposition in backswamps may lead to a more homogenous floodplain surface, which may have distinct long-term ecological implications including reductions in riparian biodiversity (Hupp et al., 2009a,b). Richter et al. (2003) argued that ecologically sustainable water management (water release scenarios) might revert the adverse hydrogeomorphic effects of regulated flows (no high flows and lengthy moderate flows) that are now focused mainly on facilitating human interests.

5.2. Deposition patterns and channel trajectory

Clear patterns occur in sediment deposition upstream to downstream on the LRR and locally along the levee to backswamp gradient. We do not believe, however, that these patterns are static; rather, they follow a trajectory in time and space (Schumm and Parker, 1973;

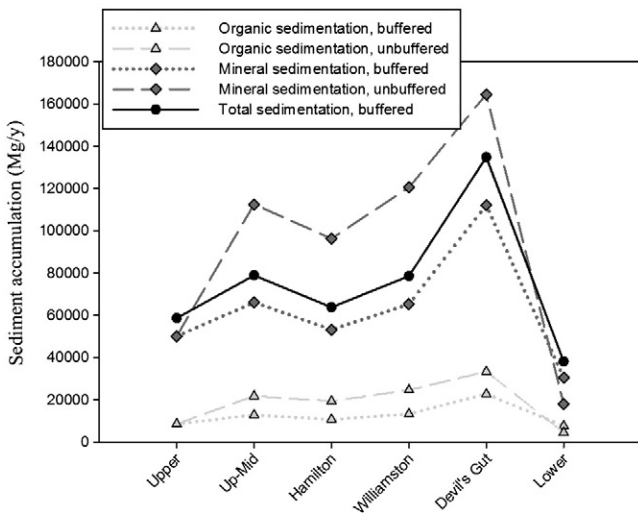


Fig. 9. Sediment accumulation rate (net) in Mg/y, separated into total, mineral, and organic components. Comparison of dotted versus dashed lines for mineral and organic material reveals the impact on sediment flux of buffering out floodplain areas >1.2 km from contributing parts of the channel.

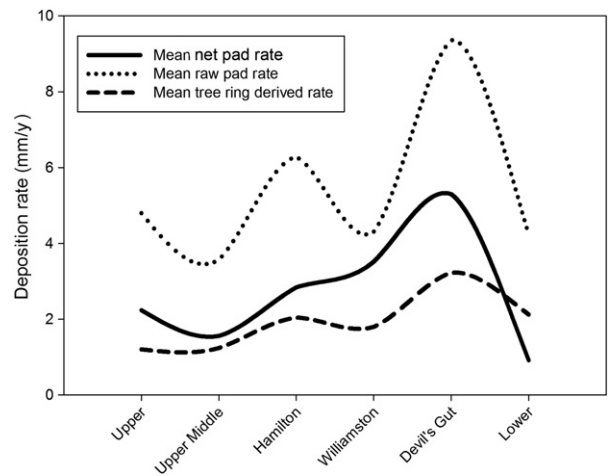


Fig. 10. Net deposition rate by segment as largely bounded by the conservative (by design) dendrogeomorphic techniques and the typically overestimating raw clay pad determined rates.

Hey, 1979) in response to the two major human interactions, legacy sedimentation and regulated flow from dams. Dendrogeomorphic and clay pad results show that backswamp and transition deposition rates (most sediment trapping) increase from upstream to downstream peaking at Devils Gut (Figs. 4 and 7) with the rates higher and peak more pronounced in the short-term clay pad data. The dendrogeomorphic results should be more muted because they cover periods pre- and post-dam closure when the sedimentation patterns were different. This is most clear in the pollen results where deposition rates were distinctly highest upstream, contrary to the two other sedimentation measurements (Fig. 7). The pollen results, also contrary to dendrogeomorphic and clay pad results, show that legacy deposition was highest on levees and markedly less on transition and backswamp features (Fig. 11). The legacy accretion pattern likely moved downstream from the Fall Line in a wave-like fashion, attenuating as it progressed during the legacy period, ending abruptly just downstream of the Williamston segment (Fig. 7). Why legacy sedimentation stopped here is not clear, although it is reasonable to speculate that it may be associated with the reach regime change from an alluvial system (watershed driven) to one nearing sea level (tide/marine driven) (Phillips, 1992a,b; Kroes et al., 2007; Hupp et al., 2009a; Ensign et al., 2014). Downstream of the Williamston segment, in addition to a reduction in channel gradient, several bank and bathymetric parameters change, including an increase in width/depth, much wider channel and floodplain, and low to nonexistent banks (Hupp et al., 2009a; Schenk et al., 2010). The wave of legacy deposition created the high levee-formed bank features (increasing upstream) that were relatively narrow laterally except where the channel is normal to the downvalley axis (transverse, Fig. 8). These wide levees are now somewhat relic features given the cessation of high (levee building/eroding) discharges associated with flow regulation and function more like alluvial fans than floodplains and even display features analogous to fan-head trenches where well developed, as in the Williamston segment.

Backswamp and, to a lesser degree, transition features have deposition rates that have remained dynamic since dam closure (Fig. 11). In fact, because of increases in bank erosion associated with regulated flow (Williams and Wolman, 1984; Grant et al., 2003; Hupp et al., 2009a), deposition in these features show an increase in recent (especially clay pad estimated) deposition rates (Figs. 6 and 11). Bank erosion on the LRR has been reported in detail (Hupp et al., 2009a, b; Schenk et al., 2010), which indicates that net bank erosion (channel widening) occurs along most of the LRR (Hupp et al., 2009a, b). This erosion

exceeds that normally expected on an equilibrated channel and demonstrates the destabilizing effects of dams on channel geomorphology in downstream reaches (Grant et al., 2003). In general, erosion rates increased from the Upper segment to the Hamilton/Williamston segments (Fig. 1), and then diminished downstream (Hupp et al., 2009a). Evidence of erosion may take the form of particle-by-particle erosion along straight and cut banks with concave upward profiles, often leaving overhanging trees and shrubs, or mass wasting through bank failures that may carry large amounts of soil partly or completely down the bank slope (Hupp, 1992). This material is subsequently entrained by flow and may form a large portion of the suspended sediment load that can be deposited on the floodplain downstream, now peaking in the backswamp of the Devils Gut segment (Fig. 4).

The increase in floodplain deposition since dam closure from the upstream segments to the Devils Gut segment (Fig. 10) may be expected given the general increases in bank erosion and mass wasting at least to the middle reaches (Hupp et al., 2009a). The present wave of destabilizing channel degradation (erosion) likely has a similar trajectory as described for legacy and post-dam deposition patterns – a probable attenuating process response (Schumm and Parker, 1973; Hey, 1979). In fact, the wave of erosion now peaking in the middle segments is the likely cause of the post-dam depositional wave. Long-term impacts of dam construction and regulated flow may have forced most of the sediment and associated material trapping to occur in low, backswamp areas of the floodplain and not on the large natural levees along the LRR, which ultimately may lead to a high floodplain with little to no topographic relief. As the floodplain surface rises in elevation relative to the widening channel, a negative feedback loop may develop such that the floodplain may trap increasingly less sediment over time. This situation appears to be in force along the relatively stable upper segments, which have a wider channel (Schenk et al., 2010) – not the typical trend on alluvial rivers – and higher banks than downstream. The upper segments presumably began eroding soon after dam completion, and presently the impetus for erosion has lessened locally and migrated downstream to the middle segments; this migration presumably pushed the floodplain deposition rate maximum to its present downstream location on the Devils Gut backswamp (Figs. 9 and 10).

5.3. GIS model analysis of floodplain sedimentation patterns

The mass of sediment trapped on the LLR floodplain (~453,000 Mg/y, Table 3) was estimated through functional floodplain segmentation

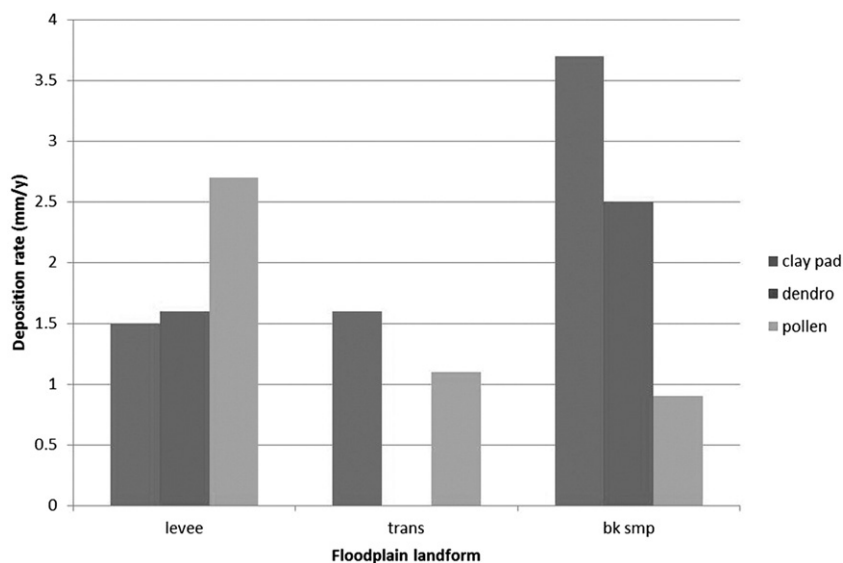


Fig. 11. Deposition rates from the three measurement approaches separated by floodplain landform. The long-term rate suggests that levees were most impacted by legacy deposition, whereas modern deposition rates are highest in the backswamp. Dendrogeomorphic data were not separated into the transition landform.

and GIS partitioning of inundation into grid codes informed by actual clay pad measurements of deposition. When combined with the areal extent of a given grid code in a segment, the estimate represents a distinct improvement from earlier trapping estimates (Hupp et al., 2009a, b). Further, these estimates have been adjusted for nonfluvial deposition and buffered for suspended sediment depletion, which may provide the most accurate accounting of sediment accumulation on floodplains in the literature to date. The downstream pattern for increasing sedimentation from upstream to downstream peaking at the Devils Gut (Fig. 9) segment is similar to that observed in relatively long-term dendrogeomorphic analyses (Fig. 10).

We observed that landforms, namely levees, with relatively high elevations and supporting dry bottomland vegetation (Townsend and Walsh, 2001; White and Peet, 2013) typically had grid codes higher than 6; whereas generally wet areas, including some transition zones, were in grid code 6 or lower. This grid code marks an overall inundation/sedimentation threshold observed along the LRR. Three-quarters of the entire floodplain is in grid code 6 or less, inundated by median discharges, and traps nearly 85% of the annual mass of deposited sediment. However, this observation varies by segment; clear differences in proportion of floodplain in the various grid codes occur (Fig. 12). The upper reaches of the LRR display a fairly even distribution of grid codes (Fig. 12A), the middle reaches show distinct reduction in proportion of floodplain in grid codes higher than 6 (Fig. 12B), and lower reaches are nearly all in grid code 4 or lower (Fig. 12C). Note that grid code 13 has been removed from analysis given that discharges in excess

of 1000 m³/s constitute <1% of the flow duration (Fig. 2) through to high areas that are not part of the functional floodplain. Landform proportions separated by grid codes also display distinct patterns. Levees (grid codes 7 and higher) systematically decline from the upstream to downstream segment while backswamps (grid codes 4 and lower) display a nearly identical but reverse trend (Fig. 13). Transition areas (grid codes 5 and 6) peak in the middle segments (Fig. 13) and may be related to the extensive legacy deposits (levee/transition areas).

Some previous studies have indicated that hydroperiod or elevation may be positively related to deposition rates (Hupp and Bazemore, 1993). Others have suggested distance from the main channel may be negatively related to deposition (Hobo et al., 2010). Still others (Heimann and Roell, 2000; Hupp et al., 2008; Schenk et al., 2012) could not confirm a consistent relation with elevation or distance from the channel, but showed a positive relation between magnitude and duration of flow and sediment transport. All of these studies strongly indicate, in one form or another, that connectivity to sediment-laden water is key to understanding factors affecting sediment deposition (Hupp et al., 2008; Schenk and Hupp, 2009). How this connectivity is maintained may differ from river to river and site to site and presumably partly explains variation in the results among various studies.

The LRR deposition patterns by all measurements show a distinct drop in deposition in the Lower segment (Figs. 7, 9, 11) in spite of having the largest proportion of backswamp (Fig. 13) where deposition is typically greatest (Fig. 4). Clearly more is at play here than inundation duration and begs explanation. It could simply be that most suspended sediment has been scavenged by upstream depositional areas, especially the Devil's Gut Segment immediately upstream. Water clarity observations (Schenk et al., 2010) support this possibility. Stream channels, as they approach estuaries or larger rivers, may have a tendency to demonstrate greater cross sectional areas as their hydrology is increasingly dominated by the receiving water body. However, a more general regime shift typically occurs along rivers as they approach sea level (Phillips, 1995; Kroes et al., 2007; Ensign et al., 2014), where for several reasons including flow reversals associated with tides, watershed (upstream)-dominated discharges and sediments cease to be main drivers in river dynamics.

Previous research, using relatively raw clay pad measurements estimated a depositional surplus of ~2.8 million m³/y (1.3 million Mg/y) (Hupp et al., 2009a). The measured sediment trapping throughout the LRR after considerable adjustment in the present paper (0.45 million Mg/y) reduced the total sediment trapping by an order of magnitude. Both estimates, still, far exceed estimated sediment sources. Fluvial, or particle by particle erosion, may account for 55,000 Mg/y (Hupp et al., 2009a) and another 84,000 Mg/y has been measured as suspended sediment at the Roanoke Rapids USGS stream gage just downstream of the dam (Schenk et al., 2010). Mass wasting on banks may account for a large part of suspended sediment in transport (Hupp, 1992) and was identified as a probable major source on the LRR (Hupp et al., 2009a). This bank erosion process has not been adequately measured here or along many streams in general. Erosion of levees, including relic features, through crevasses and internal drainage and wind-borne material may also be sediment sources. The development of a relatively accurate sediment budget for the LRR is not within the scope of the present paper. However, among previous bank erosion, bathymetric, and preliminary turbidity analyses (Hupp et al., 2009a; Schenk et al., 2010) and the results from this paper a reasonable sediment budget is within reach. Remaining efforts would need an assessment and quantification of in-channel sediment dynamics (including mass wasting on banks) and a more complete/quantitative analysis of suspended sediment or a surrogate throughout the LRR.

6. Conclusions

The floodplain of the LRR has experienced considerable alterations in hydrogeomorphic processes, especially patterns of sediment deposition, since the early 1700s. The alterations resulted from two human

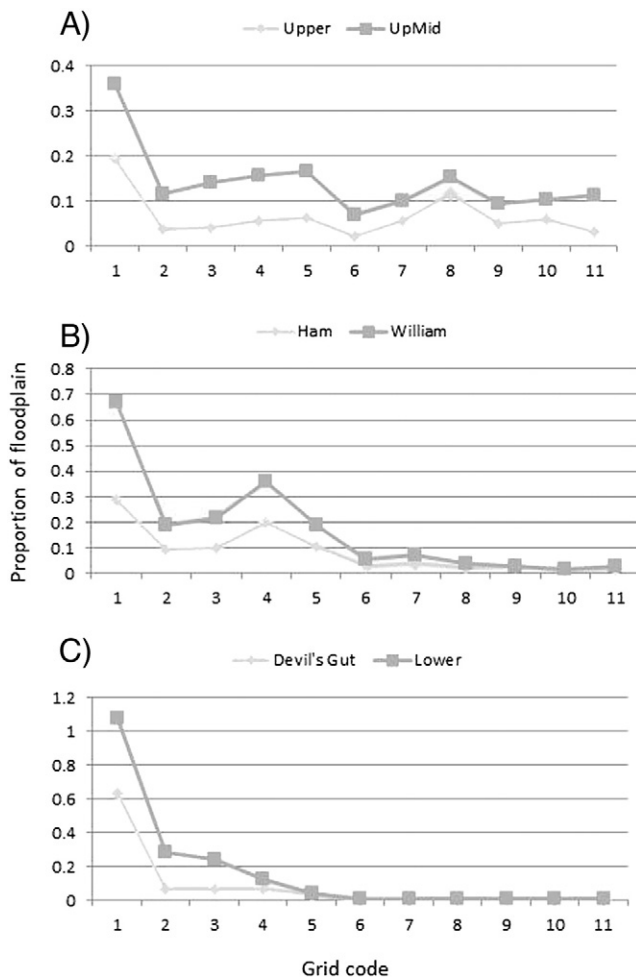


Fig. 12. Proportion of floodplain in the various grid codes separated by the six river segments, shown in paired adjacent segments: (A) upper part of study area; (B) middle part of study area; (C) lower part of study area. Note similarity of trends in the paired lines in each of the three groupings from upstream (A) to downstream (C).

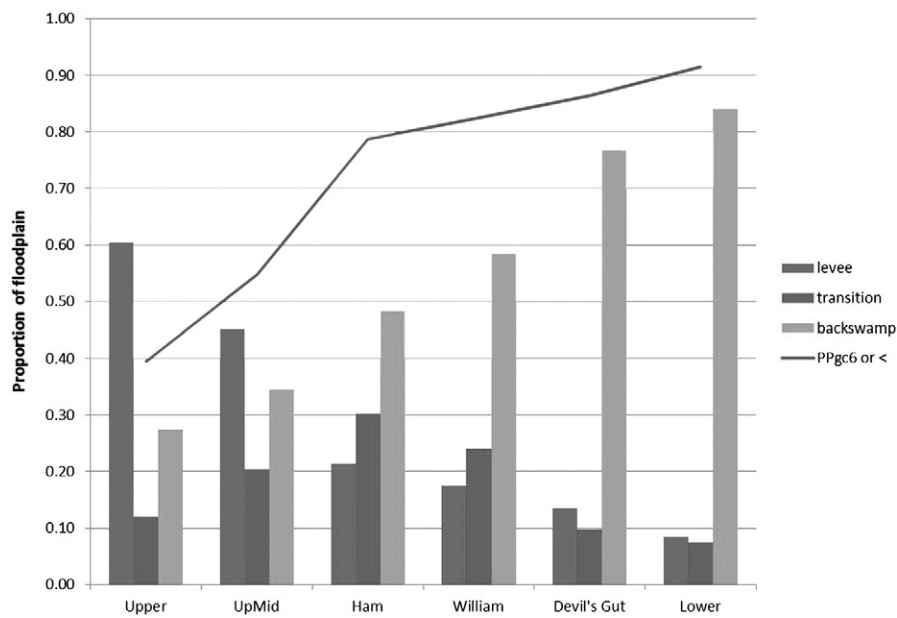


Fig. 13. Proportion of floodplain in levee, transition, and backswamp areas by river segment (columns). Line (PPgc6 or <) indicates the proportion of floodplain in grid code 6 or lower (wetter). Levees display a consistent decrease in proportion from upstream to downstream; the converse is displayed for backswamps, while transition areas peak at the Hamilton and Williamston segments where wide levee/transition landforms occur. This part of the channel also marks a distinct break in slope of the grid code 6 trend.

impacts: upland erosion upstream of the Fall Line associated with post-colonial agricultural practices leading to high deposition rates downstream and from the construction of high dams on the Piedmont near the Fall Line that severely limit the normal range of discharges typical on nonregulated rivers. Together, these alterations affect most aspects of present fluvial sedimentation dynamics along the lower river where legacy deposits in banks are the greatest source of suspended sediment in stream flow, which is tightly regulated by discharges from dams.

The comparison of deposition rates determined from different techniques allow for analysis at three time scales; annual through clay pad analysis, decadal through dendrogeomorphic analysis, and centennial through pollen analysis. Annual and decadal sedimentation rates, encompassing the period since dam closure, increase downstream peaking in the lower third of the LRR and sediment is accumulating mostly in transition and backswamp areas. Whereas, centennial sedimentation rates since the beginning of colonial agriculture upstream through the nineteenth century were highest in the upper parts of the river and were largely a levee/transition forming process; these rates diminish where the modern rates increase. The lowest segment of the river has not received considerable sediment from watershed sources during any studied time period and may represent the location of a regime shift associated with elevations near sea level (wind tides in the case of the LRR). Dendrogeomorphic cohort analyses indicate that deposition rates in the upper half of the LRR have remained similar since about 1850 but substantially increased in the lower half of the river since dam closure in 1953, especially in backswamp areas. Additionally, pollen analysis in combination with tree-ring information suggests that the high accretion rates associated with post-colonial agriculture occurred between about 1725 and 1850. The present and legacy periods of floodplain sedimentation sustained maxima that migrated from upstream to downstream and attenuated with distance from the Fall Line as process-response fluvial phenomena. These waves of sedimentation may be analogous to that of prograding deltaic processes.

The GIS model analysis of floodplain sedimentation predicts a substantial surplus of deposited material. However, the overestimation of sediment trapping is much less than that reported for the Mid-Atlantic region in general (Noe and Hupp, 2009) and the LRR in specific (Hupp et al., 2009a, b). Clay pad information that has been adjusted for autochthonous (nonfluvial) deposition, buffered to remove areas distant from

sediment-laden water, and separated into GIS coded elevation (inundation) intervals may provide the best estimates, to date, of floodplain sediment trapping. These deposition estimates in combination with bank erosion estimates and suspended sediment information may ultimately help provide an accurate sediment budget for the LRR and may serve as a model for similar efforts on other rivers. Sediment budget information on coastal rivers will become increasingly important in the face of sea level rise.

Acknowledgements

This study was part of a larger effort funded in part by NSF grant EAR GEO 0105929, the USGS National Research Program, the USGS Climate and Land Use Change Research and Development Program, The Nature Conservancy (TNC), and the U.S. Fish and Wildlife Service. The number of people who assisted in this research, in the field and in the lab, is large and would be impossible to recognize all. However, the authors would like to thank Mike Schening, Randy Richardson, Mike Shackelford, Josh Elwell, Tommy Donnelson, and Russ Gray for many long days in the field and laboratory. We would like to recognize former TNC staff Jeff Horton and Sam Pearsall for assistance and support in the early days; Jean Richter (USFWS) for her generosity and help in field logistics; Tom Sheehan for pollen processing; Bryan Landacre, Roger Brown, and Chris Bernhardt for assistance in pollen analyses and helpful discussion; and especially Jackie White (recent UNC Ph.D.) for verification and modifications of the GIS inundation model and recent clay pad measurements. Waite Osterkamp provided valuable colleague review. Suggestions provided by anonymous peers and the editor, Richard Marston, further improved the clarity of the manuscript. And lastly, we appreciate the work of many fine researchers too numerous to name except through citation in the present paper.

References

- Aust, W.M., McKee, S.E., Seller, J.R., Strahm, B.D., Schilling, E.B., 2012. Long-term sediment accretion in bottomland hardwoods following timber harvest disturbances in the Mobile-Tensaw River Delta, Alabama, USA. *Wetlands* <http://dx.doi.org/10.1007/s13157-012-0318-4>.
- Bauman, R.H., Day Jr., J.W., Miller, C.A., 1984. Mississippi deltaic wetland survival: sedimentation versus coastal submergence. *Science* 224, 1093–1095.

- Bazzaz, F.A., 1974. Ecophysiology of *Ambrosia artemisiifolia*, a successional dominant. *Ecology* 55, 112–119.
- Brown, P.M., Miller, J.A., Swain, F.M., 1972. Structural and stratigraphic framework, and spatial distribution of permeability of the Atlantic Coastal Plain. U.S. Geological Survey Professional Paper 796, p. 70.
- Brush, G.S., 1984. Patterns of recent sediment accumulation in Chesapeake Bay (VA, MD, U.S.A.) tributaries. *Chem. Geol.* 44, 227–242.
- Costa, J.E., 1975. Effects of agriculture on erosion and sedimentation in the Piedmont Province, Maryland. *Geol. Soc. Am. Bull.* 86, 1281–1286.
- Craft, C.B., 2007. Freshwater input structures soil properties, vertical accretion, and nutrient accumulation on Georgia and U.S. tidal marshes. *Limnol. Oceanogr.* 52, 1220–1230.
- Craft, C.B., Casey, W.P., 2000. Sediment and nutrient accumulation in floodplain and depressional freshwater wetlands of Georgia, USA. *Wetlands* 20, 323–332.
- Ensign, S.H., Noe, G.B., Hupp, C.R., 2014. Linking channel hydrology with riparian wetland accretion in tidal rivers. *J. Geophys. Res. Earth Surf.* 119. <http://dx.doi.org/10.1002/2013JF002737>.
- Fisk, H.N., 1952. Geological Investigation of the Atchafalaya Basin and the Problem of Mississippi River Diversion. Waterways Experiment Station, Vicksburg, MS, USA.
- Friedman, J.M., Osterkamp, W.R., Lewis, W.M., 1996. The role of vegetation and bed-level fluctuations in the process of channel narrowing. *Geomorphology* 14, 341–351.
- Grant, G.E., Schmidt, J.C., Lewis, S.L., 2003. A geological framework for interpreting downstream effects of dams on rivers. In: O'Connor, J.E., Grant, G.E. (Eds.), *A Peculiar River: American Geophysical Union. Water Science and Application* 7, pp. 209–225.
- Guy, H.P., 1969. Laboratory Theory and Methods for Sediment Analysis. U.S. Geological Survey Techniques of Water-Resources Investigation, Book 5. (Chapter C1, 58 pp.).
- Heath, S.K., Plater, A.J., 2010. Records of pan (floodplain wetland) sedimentation as an approach for post-hoc investigation of the hydrological impacts of dam impoundment: the Pongolo River, KwaZulu-Natal. *Water Res.* 44, 4226–4240.
- Heimann, D.C., Roell, M.J., 2000. Sediment loads and accumulation in a small riparian wetland system in northern Missouri. *Wetlands* 20, 219–231.
- Hey, R.D., 1979. Flow resistance in gravel-bed rivers. *J. Hydraul. Div.* 105, 365–379.
- Hobo, N., Makaske, B., Middelkoop, H., Wallinga, J., 2010. Reconstruction of floodplain sedimentation rates: a combination of methods to optimize estimates. *Earth Surf. Process. Landf.* 35, 1499–1515.
- Hupp, C.R., 1992. Riparian vegetation recovery patterns following stream channelization: a geomorphic perspective. *Ecology* 73, 1209–1226.
- Hupp, C.R., 1999. Relations among riparian vegetation, channel incision processes and forms, and large woody debris. In: Darby, S.E., Simon, A. (Eds.), *Incised River Channels*. John Wiley and Sons, Chichester, UK, pp. 219–245.
- Hupp, C.R., 2000. Hydrology, geomorphology, and vegetation of Coastal Plain rivers in the southeastern United States. *Hydrol. Process.* 14, 2991–3010.
- Hupp, C.R., Bazemore, D.E., 1993. Temporal and spatial aspects of sediment deposition in West Tennessee forested wetlands. *J. Hydrol.* 141, 179–196.
- Hupp, C.R., Bornette, G., 2003. Vegetation as a tool in the interpretation of fluvial geomorphic processes and landforms in humid temperate areas. In: Kondolf, M., Piegay, H. (Eds.), *Tools in Geomorphology*. John Wiley and Sons, UK, pp. 269–288.
- Hupp, C.R., Osterkamp, W.R., 1996. Riparian vegetation and fluvial geomorphic processes. *Geomorphology* 14, 277–295.
- Hupp, C.R., Woodside, M.D., Yanosky, T.M., 1993. Sediment and trace element trapping in a forested wetland, Chickahominy River, Virginia. *Wetlands* 13, 95–104.
- Hupp, C.R., Demas, C.R., Kroes, D.E., Day, R.H., Doyle, T.W., 2008. Recent sedimentation patterns within the central Atchafalaya Basin, Louisiana. *Wetlands* 28, 125–140.
- Hupp, C.R., Schenk, E.R., Richter, J.M., Peet, R.K., Townsend, P.A., 2009a. Bank erosion along the dam regulated lower Roanoke River, North Carolina. *Geol. Soc. Am. Spec. Publ.* 451, 97–108.
- Hupp, C.R., Pierce, A.R., Noe, G.B., 2009b. Floodplain geomorphic processes and environmental impacts of human alteration along Coastal Plain rivers, USA. *Wetlands* 29, 413–429.
- Jackson, C.R., Martin, J.K., Leigh, D.S., West, L.T., 2005. A southeastern Piedmont watershed sediment budget: evidence of a multi-millennial agricultural legacy. *J. Soil Water Conserv.* 60, 298–310.
- Jacobson, R.B., Coleman, D.J., 1986. Stratigraphy and recent evolution of Maryland Piedmont flood plains. *Am. J. Sci.* 286, 617–637.
- James, L.A., 2013. Legacy sediment: definitions and processes of episodically produced anthropogenic sediment. *Anthropocene* 2, 16–26.
- Jolley, R.L., Lockaby, B.G., Cavalcanti, G.G., 2010. Changes in riparian forest composition along a sedimentation rate gradient. *Plant Ecol.* 210, 317–330.
- Keever, C., 1983. A retrospective view of old-field succession after 35 years. *Am. Midl. Nat.* 110, 397–404.
- Kleiss, B.A., 1996. Sediment retention in a bottomland hardwood wetland in eastern Arkansas. *Wetlands* 16, 321–333.
- Knox, J.C., 2006. Floodplain sedimentation in the Upper Mississippi Valley: natural versus human accelerated. *Geomorphology* 79, 286–310.
- Kroes, D.E., Hupp, C.R., 2010. The effect of channelization on floodplain sediment deposition and subsidence along the Pocomoke River, Maryland. *J. Am. Water Resour. Assoc.* 46, 686–698.
- Kroes, D.E., Hupp, C.R., Noe, G.B., 2007. Sediment, nutrient, and vegetation trends along the tidal, forested Pocomoke River, Maryland. In: Conner, W.H., Doyle, T.W., Krauss, K.W. (Eds.), *Ecology of Tidal Freshwater Forested Wetlands of the Southeastern United States*. Springer, Netherlands, pp. 113–137.
- Meade, R.H., 1982. Sources, sinks, and storage of river sediment in the Atlantic drainage of the United States. *J. Geol.* 90, 235–252.
- Middelkoop, H., Van der Perk, M., 1998. Modelling spatial patterns of overbank sedimentation on embanked floodplains. *Geogr. Ann.* 80A, 95–109.
- Moulin, B., Schenk, E.R., Hupp, C.R., 2011. Distribution and characterization of in-channel large wood in relation to geomorphic patterns on a low-gradient river. *Earth Surf. Process. Landf.* 36, 1137–1151.
- Nanson, G.C., Croke, J.C., 1992. A genetic classification of floodplains. *Geomorphology* 4, 459–486.
- Nelson, D.W., Sommers, L.E., 1996. Total carbon, organic carbon, and organic matter. In: Sparks, D.L. (Ed.), *Methods of Soil Analysis Part 3—Chemical Methods*. Soil Science Society of America, Inc, Madison, WI, USA, pp. 961–1010.
- Nilsson, C., Reidy, C.A., Dynesius, M., Revenga, C., 2005. Fragmentation and flow regulation of the world's large river systems. *Science* 308, 405–408.
- Noe, G.B., Hupp, C.R., 2009. Retention of riverine sediment and nutrient loads by Coastal Plain floodplains. *Ecosystems* 12, 728–746.
- Osterkamp, W.R., Hupp, C.R., 1984. Geomorphic and vegetative characteristics along three northern Virginia streams. *Bull. Geol. Soc. Am.* 95, 501–513.
- Osterkamp, W.R., Hupp, C.R., 2010. Fluvial processes and vegetation — glimpses of the past, the present, and perhaps the future. *Geomorphology* 116, 274–285.
- Pearsall, S.H., McCrodden, B.J., Townsend, P.A., 2005. Adaptive management of flows in the lower Roanoke River, North Carolina, USA. *Environ. Manag.* 35, 353–367.
- Phillips, J.D., 1992a. The source of alluvium in large rivers of the lower Coastal Plain of North Carolina. *Catena* 19, 59–75.
- Phillips, J.D., 1992b. Delivery of upper-basin sediment to the lower Neuse River, North Carolina, USA. *Earth Surf. Process. Landf.* 17, 699–709.
- Phillips, J.D., 1995. Decoupling of sediment sources in large river basins. In: Osterkamp, W.R. (Ed.), *Effects of scale on Interpretation and Management of Sediment and Water Quality*. IAHS Publication 226, pp. 11–16.
- Phillips, J.D., 1997. Human agency, Holocene sea level, and floodplain accretion in Coastal Plain rivers. *J. Coast. Res.* 13, 854–866.
- Piegay, H., Hupp, C.R., Citterio, A., Dufour, S., Moulin, B., Walling, D.E., 2008. Spatial and temporal variability in sedimentation rates associated with cutoff channel infill deposits: Ain River, France. *Water Resour. Res.* 44, W05420. <http://dx.doi.org/10.1029/2006WR005260>.
- Pizzuto, J.E., 1987. Sediment diffusion during overbank flows. *Sedimentology* 34, 301–317.
- Raymond, P.A., Bauer, J.E., 2001. Riverine export of aged terrestrial organic matter to the North Atlantic Ocean. *Nature* 409, 497–500.
- Richter, B.D., Baumgartner, J.V., Powell, J., Braun, D., 1996. A method for assessing hydrologic alteration within ecosystems. *Conserv. Biol.* 10, 1153–1174.
- Richter, B.D., Mathews, D.R., Harrison, D.L., Wigington, R., 2003. Ecologically sustainable water management: managing river flows for ecological integrity. *Ecol. Appl.* 13, 206–224.
- Ross, K.M., Hupp, C.R., Howard, A.D., 2004. Sedimentation in floodplains of selected tributaries of the Chesapeake Bay. In: Bennett, S.J., Simon, A. (Eds.), *Riparian Vegetation and Fluvial Geomorphology*. American Geophysical Union, Water Science and Applications 8, pp. 187–208.
- Schenk, E.R., Hupp, C.R., 2009. Legacy effects of colonial millponds on floodplain sedimentation, bank erosion, and channel morphology, Mid-Atlantic, USA. *J. Am. Water Resour. Assoc.* 45, 597–606.
- Schenk, E.R., Hupp, C.R., Richter, J.M., Kroes, D.E., 2010. Bank erosion, mass wasting, water clarity, bathymetry, and a sediment budget along the dam-regulated lower Roanoke River, North Carolina. U.S. Geological Survey Open File Report 2009–1260 (12 p.).
- Schenk, E.R., Hupp, C.R., Gellis, A., 2012. Sediment dynamics in the restored reach of the Kissimmee River Basin, Florida: a vast subtropical riparian wetland. *River Res. Appl.* 28, 1753–1767.
- Schmidt, J.C., Wilcock, P.R., 2008. Metrics for assessing the downstream effects of dams. *Water Resour. Res.* 44, W04404. <http://dx.doi.org/10.1029/2006WR005092>.
- Schumm, S.A., Parker, R.S., 1973. Implications of complex response of drainage systems for Quaternary alluvial Stratigraphy. *Nature* 243, 99–100.
- Scott, M.L., Auble, G.T., Friedman, J.M., 1997. Flood dependency of cottonwood establishment along the Missouri River, Montana, USA. *Ecol. Appl.* 7, 677–690.
- Sigafoos, R.S., 1964. Botanical evidence of floods and flood-plain deposition. U.S. Geological Survey Professional Paper 485-A, pp. 1–35.
- Simmons, C.E., 1988. Sediment characteristics of North Carolina streams. U.S. Geological Survey Open-File Report 87–701 (130 p.).
- Steiger, J., Gurnell, A.M., Ergenzinger, P., Snelder, D., 2001. Sedimentation in the riparian zone of an incising river. *Earth Surf. Process. Landf.* 26, 91–108.
- Stockmarr, J., 1971. Tablets with spores used in absolute pollen analysis. *Pollen Spores* 13, 615–621.
- Townsend, P.A., Walsh, S.J., 1998. Modeling floodplain inundation using integrated GIS with radar and optical remote sensing. *Geomorphology* 21, 295–312.
- Townsend, P.A., Walsh, S.J., 2001. Relationships between vegetation patterns and hydroperiod on the Roanoke River floodplain, North Carolina. *Plant Ecol.* 156, 43–58.
- Townsend, P.A., Brown, R.A., Willard, D.A., Hupp, C.R., Peet, R.K., Pearsall, S.H., 2004. Ecosystem change at multiple temporal and spatial scales: linking hydrology, geomorphology and ecology on the Roanoke River floodplain, North Carolina. *Geol. Soc. Am. Abstr. Programs* 36, 141.
- Trimble, S.W., 1974. Man-induced soil erosion on the southern Piedmont, 1700–1970. *Soil Conservation Society of America, Ankeny, Iowa* 180 pp.
- Trimble, S.W., 1983. A sediment budget for Coon Creek basin in the Driftless Area, Wisconsin, 1853–1977. *Am. J. Sci.* 283, 454–474.
- Tye, R.S., Coleman, J.H., 1989. Evolution of Atchafalaya lacustrine deltas, south-central Louisiana. *Sediment. Geol.* 65, 95–112.
- Walling, D.E., He, Q., 1998. The spatial variability of overbank sedimentation on river floodplains. *Geomorphology* 24, 209–223.

- Walling, D.E., He, Q., Nicholas, A.P., 1996. Floodplains as suspended sediment sinks. In: Anderson, M.S., Walling, D.E., Bates, P.D. (Eds.), *Floodplain Processes*. John Wiley and Sons, Inc, Chichester, UK, pp. 399–439.
- White, J., Peet, R.K., 2013. Establishment and survival of tree seedlings in the floodplain forests of the lower Roanoke River and their relationship to variation in site hydrology. Report to Dominion Generation. Institute for the Environment, Univ. of North Carolina, Chapel Hill, NC (123 p.).
- Willard, D.A., Cronin, T.M., Verardo, S., 2003. Late-Holocene climate and ecosystem history from Chesapeake Bay sediment cores, USA. *The Holocene* 13, 201–214.
- Willard, D.A., Bernhardt, C.E., Brown, R., Landacre, B., Townsend, P.A., 2010. The Holocene <http://dx.doi.org/10.1177/0959683610378876>.
- Williams, G.P., Wolman, M.G., 1984. Downstream effects of dams on alluvial rivers. U.S. Geological Survey Professional Paper 1286.